Supplementary Material for "Information Scrambling and Loschmidt Echo"

Appendix A: Haar integral of subsystem operators

In this appendix we prove the formula in Eq. (4) in the main text.

For a single system, the Haar integral over a unitary operator A gives

$$\int dA\ A^\dagger O A = \frac{1}{d}\,\mathrm{tr}(O)\mathbb{I}. \tag{A1}$$

Here, $dA \equiv d\mu(A)$ with μ the Haar measure on a unitary group.

This is a consequence of the defining property of the Haar measure, namely, the Haar measure is invariant under the transformation $A \to AU$, i.e., $\mu(A) = \mu(AU)$, where U is an arbitrary unitary operator. This implies

$$\int d\mu(A) A^\dagger O A = U^\dagger \left(\int d\mu(A) A^\dagger O A \right) U. \tag{A2}$$

Thus, the Haar average of an operator A is proportional to the identity operator. In finite dimension, its trace can be computed as

$$\mathrm{tr} \int d\mu(A) A^\dagger O A = \int d\mu(A)\,\mathrm{tr}(O). \tag{A3}$$

The above integral is unique up to a constant multiplication factor; and the unitary groups on finite dimensional Hilbert spaces have finite measures. We can then choose $\int d\mu = 1$ as a convention. The desired property in Eq. (A1) is then deduced. We note that the identity $\int dA\ A^\dagger O A = \mathrm{tr}(O)\mathbb{I}$ holds in infinite dimensions as well. The formal mathematical treatment of the infinite dimensional case will be published elsewhere [1].

For an operator O_{AB} on a composed system, the integral over operators on a subsystem can be performed in a similar way, by performing the partial trace:

$$\begin{aligned}
&\int dA\ A^\dagger \otimes \mathbb{I}_B O_{AB} A \otimes \mathbb{I}_B \\
&= \int dA\ A^\dagger \otimes \mathbb{I}_B \sum_i O_i^A \otimes O_i^B A \otimes \mathbb{I}_B \\
&= \sum_i \int dA\ A^\dagger O_i^A A \otimes O_i^B \\
&= \frac{1}{d_A} \sum_i \mathrm{tr}(O_i^A)\mathbb{I}_A \otimes O_i^B = \frac{1}{d_A}\mathbb{I}_A \otimes \mathrm{tr}_A\, O_{AB}\ .
\end{aligned} \tag{A4}$$

Appendix B: Reduced dynamics for operator B

This appendix presents a more rigorous derivation of the reduced dynamical equation for the operator B in Eq. (7) of the main text.

The total system Hamiltonian admits a general decomposition

$$\begin{aligned}
H &= \mathbb{I}_A \otimes H_B + H_A \otimes \mathbb{I}_B + H', \\
H' &\equiv \delta \sum_{k=1}^{d_A^2} V_A^k \otimes V_B^k.
\end{aligned} \tag{B1}$$

where A denotes a small local subsystem S_A, B denotes the compliment of S_A to the total system. It is assumed that the total system is much larger than the local system S_A. d_A is the dimension of S_A. The operators $\{V_A^i\}_i$ are chosen to be Hermitian and orthonormal, with respect to the (weighted) Hilbert-Schmidt inner product, i.e.,

$$\mathrm{tr}(V_A^i V_A^j) = d_A \delta_{i,j}. \tag{B2}$$

Here, d_A is introduced as a convention to normalize the noise correlation functions (see below). If the operators $\{V_A^i\}_i$ are not normalized in this way, proper normalization factors will appear in the stochastic field as pre-factors. The operators V_B^i on S_B are also Hermitian, but their (Hilbert-Schmidt) norms are fixed and are equal to the norms of H_B. Thus, the parameter δ quantifies the relative strength of the couplings compared with H_B.

We are interested in strongly coupled systems, where the energy scales admits a hierarchy $\bar{H}_A \ll \bar{H}_I \ll \bar{H}_B$. For instance, in an N-particle system with all-to-all two-body interactions, when the subsystem S_A refers to a single particle, the energy scales of S_A, S_B, and the coupling between them, are of the order of 1, N^2 and N, respectively. Alternatively speaking, this condition means that the parameter $\delta \ll 1$; and energy scales of the subsystem S_A is much smaller than that of the global dynamics.

Consider the reduced dynamics of an operator B on the subsystem S_B after the trace-out procedure. We have,

$$B(-t) = \mathrm{tr}_A \left(e^{-iHt} \mathbb{I}_A \otimes B e^{iHt} \right). \tag{B3}$$

This can be thought of as a decoherence process, i.e., the total system is prepared in an initial (unnormalized) product state $d_A \left(\frac{I_A}{d_A} \right) \otimes B$, where the subsystem S_B is described by a "density matrix" B, and the subsystem S_A is in a thermal state with infinite temperature up to normalization. The "quantum state" B will become "mixed" with time evolution due to the presence of the couplings to subsystem S_A. When $\delta \ll 1$, the above evolution of $B(-t)$ can be expanded to the second order of δ. This corresponds to the Born-Markov approximation, which leads the effective master equation for $B(-t)$ to a Lindblad form. It is known that in this case the effective master equation can be simulated with the evolution of B under H_B without coupling to other systems [2], but subjects to a stochastic field

$$\delta \mathcal{F}(t) = \delta \sum_k l_k(t) V_B^k, \tag{B4}$$

with the correlations given by

$$\begin{aligned} &\overline{l_i(t) l_j(t-\tau)} \\ =&\mathrm{tr}(\frac{\mathbb{I}_A}{d_A} V_A^i e^{iH_A\tau} V_A^j e^{-iH_A\tau}) \\ \approx&\delta_{i,j}. \end{aligned} \tag{B5}$$

The approximation in the last step is due to the large energy hierarchy: the time scale of the dynamics of the subsystem S_A is much larger than that of $B(t)$ under consideration. Alternatively, this can be thought of as taking the zeroth order the H_A. As a consequence, the noise field $l_i(t)$ can be taken as a random constant ± 1 with equal probability. The reduced dynamics of the B operator is then given by

$$B(t) = d_A \times \overline{e^{-i(H_B+\mathcal{F})t} B e^{i(H_B+\mathcal{F})t}}, \tag{B6}$$

averaged over the stochastic field $\mathcal{F}$. Note that the pre-factor d_A is present in the above equation due to the normalization of $\mathbb{I}_A$.

As the noise fields are random ± 1, each realization of the stochastic field, denoted as V_α, always appears as linear combination of V_B^i's, whose coefficients take values ± 1 randomly. The noisy evolution of $B(-t)$ is then given by

$$B(-t) \approx d_A \times \frac{1}{N} \sum_{\alpha=1}^{N} e^{-i(H_B+\delta V_\alpha)t} B e^{i(H_B+\delta V_\alpha))t}, \tag{B7}$$

where N is the number of different realizations of the noise field.

Appendix C: OTOC - LE connection

This appendix presents the derivation of Eq. (9) in the main text. It has been shown in the main text that after performing averaging over operator A, the OTOC reads

$$\begin{aligned} &\int dA \; F_{\beta=0}(t) \equiv \frac{1}{d} \int dA \;\; \mathrm{tr}(A^\dagger(t) B^\dagger A(t) B) \\ =&\frac{1}{d} \frac{1}{d_A} \mathrm{tr}_B[\mathrm{tr}_A(e^{-iHt} B^\dagger e^{iHt}) \, \mathrm{tr}_A(e^{-iHt} B e^{iHt})]. \end{aligned} \tag{C1}$$

Replacing the reduced dynamics of operator B with its alternative expression Eq. (B7) allows us to further evaluate the average over all unitary operators on subsystem S_B:

$$\begin{aligned}
&\overline{F_{\beta=0}(t)}\\
=&\frac{1}{d}\frac{1}{d_A}\int dB\ \ \mathrm{tr}_B[\mathrm{tr}_A(e^{-iHt}B^\dagger e^{iHt})\,\mathrm{tr}_A(e^{-iHt}Be^{iHt})]\\
\approx&\frac{d_A}{d}\frac{1}{N^2}\sum_{\alpha,\alpha'=1}\mathrm{tr}\int dB\ e^{-i(H_B+V_\alpha)t}B^\dagger e^{i(H_B+V_\alpha)t}\times\\
&\qquad\times e^{-i(H_B+V_{\alpha'})t}Be^{i(H_B+V_{\alpha'})t}\\
=&\frac{1}{N^2}\sum_{\alpha,\alpha'=1}|\frac{1}{d_B}\mathrm{tr}(e^{i(H_B+V_\alpha)t}e^{-i(H_B+V_{\alpha'})t})|^2\\
=&\overline{|\langle e^{i(H_B+V_\alpha)t}e^{-i(H_B+V_{\alpha'})t}\rangle_{\beta=0}|^2}.
\end{aligned}\tag{C2}$$

This is Eq. (9a) in the main text.

The above equation can be generalized to finite temperatures, by distributing the operators at equal spacing around the thermal circle. Namely, let us define

$$y^4=\frac{1}{Z}e^{-\beta H},\tag{C3}$$

and evaluate the OTOC as

$$F(t)=\mathrm{tr}[yA^\dagger(t)yB^\dagger yA(t)yB].\tag{C4}$$

By absorbing the inverse temperature into the time evolution operator, the OTOC can be evaluated in the same manner as in the infinite temperature case, but in the complex time domain, $t-i\beta/4$. The averaged OTOC is translated to an infinite temperature average of LE in complex time, which is further reduced to a finite temperature average of the regular LE in real time. More precisely (using Eq. (9b) in the main text),

$$\begin{aligned}
\overline{F_\beta(t)}\approx&\left|\langle e^{i(H_B+V_1)(t+i\beta/4)}e^{-i(H_B+V_2)(t-i\beta/4)}\rangle\right|^2\\
=&\frac{1}{Z_\beta}\frac{1}{d_B^2}\left|\mathrm{tr}\,e^{i(H_B+V_1)t}e^{-\frac{\beta}{2}(H_B+O(V_1,V_2))}e^{-i(H_B+V_2)t}\right|^2\\
\approx&\frac{Z_{\beta/2}^2}{Z_\beta}\left|\langle e^{i(H_B+V_1)t}e^{-i(H_B+V_2)t}\rangle_{\beta/2}\right|^2.
\end{aligned}\tag{C5}$$

Here $O(V_1,V_2)$ is an operator resulting from the Baker-Campbell-Hausdorff expansion that contains terms involving the perturbation operators V_1 and V_2. This term is time-independent and only contributes to a vanishing correction of the thermal state. Note that the effective inverse temperature for the LE is $\beta/2$. The factor $Z_{\beta/2}^2/Z_\beta$ appears because of the particular regularization (C4). As a consequence, the OTOC at $t=0$ has a non-unit value, even for unitary operators A and B, in contrast to the regular thermal average scheme, where the OTOC at $t=0$ is unit for unitary operators. In our numerical simulations, as a convention, OTOCs are always normalized by removing this prefactor.

It is worth emphasizing that the Haar averaged OTOC is upper-bounded in the half strip $0<t$ and $-\frac{\beta}{4}\le\tau\le\frac{\beta}{4}$ for the complex time $t+i\tau$. The fact that the OTOC in this domain is bounded is crucial for the upper bound of the OTOC growth rate [3, 4]. To see this fact, consider the averaged OTOC in complex time,

$$\begin{aligned}
\overline{F_\beta(t)}\approx&\left|\langle e^{i(H_B+V_1)(t+i\tau+i\beta/4)}e^{-i(H_B+V_2)(t+i\tau-i\beta/4)}\rangle\right|^2\\
=&\frac{1}{Z_\beta}\frac{1}{d_B^2}\left|\mathrm{tr}\,e^{i(H_B+V_1)t}e^{-(\beta/4+\tau)(H_B+V_1)}e^{-(\beta/4-\tau)(H_B+V_2)}e^{-i(H_B+V_2)t}\right|^2,
\end{aligned}\tag{C6}$$

which is a bounded quantity for the effective positive temperature $\beta/4\pm\tau$.

Appendix D: OTOC and LE for the inverted harmonic oscillator

In this section, we give the details for the derivation of the OTOC and LE for the inverted harmonic oscillator.

1. Wavefunction of the IHO

The Hamiltonian of two coupled inverted harmonic oscillators (IHO) reads

$$\sum_{i=1,2}\left(\frac{1}{2m_i}\hat{p}_i^2+\frac{m_i\omega_i^2}{2}x_i^2\right)+\delta\hat{x}_1\hat{x}_2. \tag{D1}$$

Here, for convenience, the frequencies are written as imaginary numbers. This Hamiltonian is reduced to the one of two uncoupled harmonic oscillators by the following transformation,

$$\begin{aligned} x_1&=\frac{1}{\sqrt{2}}\left(y_1+y_2\right),\\ x_2&=\frac{1}{\sqrt{2}}\left(\eta y_1-\xi y_2\right), \end{aligned} \tag{D2}$$

where η are ξ are given by

$$\begin{aligned} \eta&=\left(\sqrt{D^2+4m_1/m_2}+D\right)/2,\\ \xi&=\left(\sqrt{D^2+4m_1/m_2}-D\right)/2,\\ D&=\left(\omega_1^2-\omega_2^2\right)m_1/\delta. \end{aligned} \tag{D3}$$

In the new coordinates, the effective masses and frequencies are given by

$$\begin{aligned} \widetilde{m}_1&=\frac{\left(\eta+\xi\right)^2}{2}\frac{m_1m_2}{m_1+\xi^2m_2},\\ \widetilde{m}_2&=\frac{\left(\eta+\xi\right)^2}{2}\frac{m_1m_2}{m_1+\eta^2m_2},\\ \widetilde{m}_1\widetilde{\omega}_1^2&=\left(m_1\omega_1^2+\eta^2m_2\omega_2^2+\delta\eta\right),\\ \widetilde{m}_2\widetilde{\omega}_2^2&=\left(m_1\omega_1^2+\xi^2m_2\omega_2^2+\delta\xi\right). \end{aligned} \tag{D4}$$

The regularized thermal state evolved in the OTOC and LE is replaced with a pure product state (up to a normalization factor) $|\psi(x_1)\rangle|\psi(x_2)\rangle=e^{-x_1/m_2}e^{-x_2/m_1}$. The choice of this wavefunction is not physically essential for the OTOC and LE. It is however important from a practical point of view. This particular form of wavefunction is separable in the new coordinates y_1 and y_2, which makes solving the time-dependent wavefunction much easier.

For a given initial state $\psi(x)$ of a single IHO with mass m and frequency ω, the time-dependent wavefunction can be expressed by a path integral

$$\psi(x,t)=\int dx'\ K(x,x',t,0)\psi(x',0), \tag{D5}$$

where the propagator is

$$\begin{aligned} K(x,x',t,0)=&\sqrt{\frac{m\omega}{2\pi i\sin(\omega t)}}\\ &\times\exp\left[\frac{im\omega}{2\sin\omega t}\left((x^2+x'^2)\cos\omega t-2xx'\right)\right]. \end{aligned} \tag{D6}$$

With these toolkits, the wavefunction $\psi(x_1,x_2,t)$ (which is involved in the OTOC evaluation; see the following section) can be expressed in the new coordinates using the single IHO propagator and then transfer back to the original coordinates.

2. Haar averaged OTOC for the IHO

In this section, we compute the Haar averaged OTOC for the IHO:

$$\overline{F(t)} = \int_{Haar} dAdB\, \mathrm{tr}[A^\dagger(t)\rho^{\frac{1}{4}}B^\dagger\rho^{\frac{1}{4}}A(t)\rho^{\frac{1}{4}}B\rho^{\frac{1}{4}}]. \tag{D7}$$

The operators A and B to be averaged are unitary operators on the first and second IHO, respectively. Since a termal state of the IHO is not well defined, we replace the regularized thermal state ρ_β with a pure state of the coupled IHO, i.e., $\rho(x_1,x_2;x_1',x_2') = \psi^*(x_1,x_2)\psi(x_1',x_2') = \rho^{\frac{1}{4}}(x_1,x_2;x_1',x_2')$. Using the property of the Haar measure described in Appendix A, the integral can be computed directly:

$$\begin{aligned}
&\int_{Haar} dAdB\ A^\dagger(t)\rho B^\dagger\rho A(t)\rho B\rho \\
&= \int dAdB\ A^\dagger e^{-iHt}\rho B^\dagger\rho e^{iHt}Ae^{-iHt}\rho B\rho e^{iHt} \\
&= \int dB\ \ \mathrm{tr}_A[e^{-iHt}\rho B^\dagger\rho e^{iHt}]\times e^{-iHt}\rho B\rho e^{iHt} \\
&= \int dB\ \ \int dx_1\langle x_1|e^{-iHt}\rho B^\dagger\rho e^{iHt}|x_1\rangle e^{-iHt}\rho B\rho e^{iHt} \\
&= \int dx_1\langle x_1|e^{-iHt}\rho\times \mathrm{tr}_B\left(\rho e^{iHt}|x_1\rangle e^{-iHt}\rho\right)\times\rho e^{iHt} \\
&= \int dx_1\langle x_1|e^{-iHt}\rho\langle x_2|\rho e^{iHt}|x_1\rangle e^{-iHt}\rho|x_2\rangle\times\rho e^{iHt} \\
&= \int dx_1dx_2\ \underbrace{\langle x_1|e^{-iHt}\rho}_{a}\underbrace{\langle x_2|\rho e^{iHt}|x_1\rangle}_{b}\underbrace{e^{-iHt}\rho|x_2\rangle}_{c}\underbrace{\rho e^{iHt}}_{d}
\end{aligned} \tag{D8}$$

Using the expression for the density operator, i.e.,

$$e^{-iHt}\rho = \int dx_1'dx_1''dx_2'dx_2''\ \ \psi^*(x_1',x_2',t)\psi(x_1'',x_2'')|x_1',x_2'\rangle\langle x_1'',x_2''|, \tag{D9}$$

the four terms in the above Haar integral can be evaluated separately as

$$\begin{aligned}
a &= \int dx_1''dx_2'dx_2''\psi^*(x_1,x_2',t)\psi(x_1'',x_2'')|x_2'\rangle\langle x_1'',x_2''|, \\
b &= \int dx_1''dx_2'\psi(x_1,x_2',t)\psi^*(x_1'',x_2)|x_1''\rangle\langle x_2'|, \\
c &= \int dx_1'dx_1''dx_2'\psi^*(x_1',x_2',t)\psi(x_1'',x_2)|x_1',x_2'\rangle\langle x_1''|, \\
d &= \int dx_1'dx_1''dx_2'dx_2''\ \ \psi(x_1',x_2',t)\psi^*(x_1'',x_2'')|x_1'',x_2''\rangle\langle x_1',x_2'|.
\end{aligned} \tag{D10}$$

Besides the above Haar integral, the OTOC Eq. (D7) involves a total trace, i.e.,

$$\mathrm{tr}\bullet = \int dx_1dx_2\langle x_1|\langle x_2|\bullet|x_1\rangle|x_2\rangle. \tag{D11}$$

After evaluating the trace and Haar integral, the OTOC finally reads

$$\begin{aligned}
\overline{F(t)} &= \int dx_1dx_1'dx_2dx_2'\ \ \psi(x_1,x_2,t)\psi^*(x_1',x_2,t)\psi(x_1',x_2',t)\psi^*(x_1,x_2',t) \\
&= \int dx_2dx_2'\ \rho_2(x_2',x_2)\rho_2(x_2',x_2) \\
&= \int dx_2dx_2'\ \rho_2^*(x_2,x_2')\rho_2(x_2',x_2) \\
&= \int dx_2\rho_2^2(x_2) = \mathrm{tr}(\rho_2^2).
\end{aligned} \tag{D12}$$

Here, ρ_2 is the reduce density matrix of the second oscillator. The above equation is an exact result. In this particular setting, where the regularized thermal state is replaced with a pure state, the OTOC is precisely equal to the purity of one subsystem. The purity can be computed exactly as well, using the procedure described in the previous section.

3. *Baker-Campbell-Hausdorff* expansion of the LE

In this section we derive the second order expansion with respect to the perturbation strength δ for the Loschmidt echo of the type

$$M(t) = |\langle\psi|e^{i(H-\delta\hat{x})t}e^{-i(H+\delta\hat{x})t}|\psi\rangle|^2, \tag{D13}$$

where H is the Hamiltonian of a single IHO

$$H = \frac{1}{2m}\hat{p}^2 + \frac{m\omega^2}{2}\hat{x}^2. \tag{D14}$$

Here ω is a pure imaginary number. Treating $H_0 \equiv H - \delta\hat{x}$ as the "unperturbed" Hamiltonian, the echo operator reads

$$\hat{U}_t \equiv e^{i(H-\delta\hat{x})t}e^{-i(H+\delta\hat{x})t} = e^{iH_0t}e^{-i(H_0+\delta 2\hat{x})t}. \tag{D15}$$

It can be expanded to the second order in δ using the *Baker-Campbell-Hausdorff* (BCH) formula [5]:

$$\hat{U}_t = \exp\left[-i\left(\Sigma(t)\delta + \frac{1}{2}\Gamma(t)\delta^2 + \dots\right)\right], \tag{D16}$$

where $\Sigma(t)$ and $\Gamma(t)$ are determined by the Heisenberg evolution of the perturbation operator, i.e., $2\hat{x}(t) \equiv e^{iH_0t}2\hat{x}e^{-iH_0t}$,

$$\begin{aligned}\Sigma(t) &= \int_0^t dt'\ 2\hat{x}(t') \\ \Gamma(t) &= i\int_0^t dt' \int_{t'}^t dt''\ [2\hat{x}(t'), 2\hat{x}(t'')].\end{aligned} \tag{D17}$$

To solve the Heisenberg evolution of $2\hat{x}$ under Hamiltonian H_0, we perform a coordinate transformation $y = x + 2\delta/(m\omega^2)$. In the new coordinate the Hamiltonian reads

$$H_0 = \frac{1}{2m}\hat{p}^2 + \frac{m\omega^2}{2}\hat{y}^2 - \frac{2\delta^2}{m\omega^2}. \tag{D18}$$

This is a shifted harmonic oscillator Hamiltonian, for which the Heisenberg evolution of the position operator has been computed [6]:

$$\hat{y}(t) = \hat{y}\cos\omega t + \frac{1}{m\omega}\hat{p}\sin\omega t, \tag{D19}$$

which gives

$$\hat{x}(t) = \hat{x}\cos\omega t + \frac{1}{m\omega}\hat{p}\sin\omega t + \frac{2\delta}{m\omega^2}\left(\cos\omega t - 1\right). \tag{D20}$$

The last term in the above equation will be dropped since it contributes to higher than second-order in δ for the LE. Σ and Γ are thus given by

$$\begin{aligned}\Sigma(t) =& \frac{2}{\omega}\hat{x}\sin\omega t - \frac{2}{m\omega^2}\hat{p}\cos\omega t + \frac{2}{m\omega^2}\hat{p}, \\ \Gamma(t) =& \frac{4}{m\omega^3}\sin\omega t - \frac{4}{m\omega^2}t.\end{aligned} \tag{D21}$$

In the following, we perform a Taylor expansion of the LE to second order in δ. The second order expansion for the average of the echo operator (D15) is given by

$$\langle\psi|\hat{U}_t|\psi\rangle = 1 - i\left(\overline{\Sigma(t)}\delta + \frac{1}{2}\overline{\Gamma(t)}\delta^2\right) - \frac{1}{2}\overline{\Sigma^2(t)}\delta^2. \tag{D22}$$

Note that both $\Sigma(t)$ and $\Gamma(t)$ are real, there are only non-vanishing two second-order terms kept in the magnitude-square of the above quantity, which gives the final expression of the LE:

$$M(t) = |\langle\psi|\hat{U}_t|\psi\rangle|^2 = 1 - \left(\overline{\Sigma^2(t)} + \overline{\Sigma(t)}^2\right)\delta^2. \tag{D23}$$

As defined in the previous sections, the pure state for the OTOC average is chosen as a Gaussian form with zero mean. In this case only the first term in $\Sigma(t)$ has a non-zero contribution to the LE $M(t)$, i.e.,

$$\begin{aligned} M(t) =& 1 - \frac{\delta^2}{\omega^2}\sin^2\omega t\langle\psi|(2\hat{x})^2|\psi\rangle \\ =& 1 - \delta^2\frac{4\overline{\hat{x}^2}}{\omega^2}\sin^2\omega t. \end{aligned} \tag{D24}$$

Appendix E: Finite size study of the SYK model.

To further test our theory, we present numerical study of the fermionic version of the SYK model proposed in [7]. The Hamiltonian of the SYK model reads

$$H = \frac{1}{(2N)^{3/2}}\sum_{i,j,k,l=1}^{N} J_{i,j;k,l}c_i^\dagger c_j^\dagger c_k c_l, \tag{E1}$$

where $J_{i,j;k,l}$ are complex Gaussian random couplings with zero mean obeying certain symmetries. c_i and $c_i^\dagger$ are fermionic annihilation and creation operators at site i. We compute the OTOC for operators $c_i^\dagger + c_i$ on two distinct sites. Clear Gaussian decay with very weak temperature dependence has been observed (Fig. E.1), which agrees with previous numerical studies [7, 8] while contradicting the expected exponential decay with upper bound $2\pi/\beta$ [3, 4].

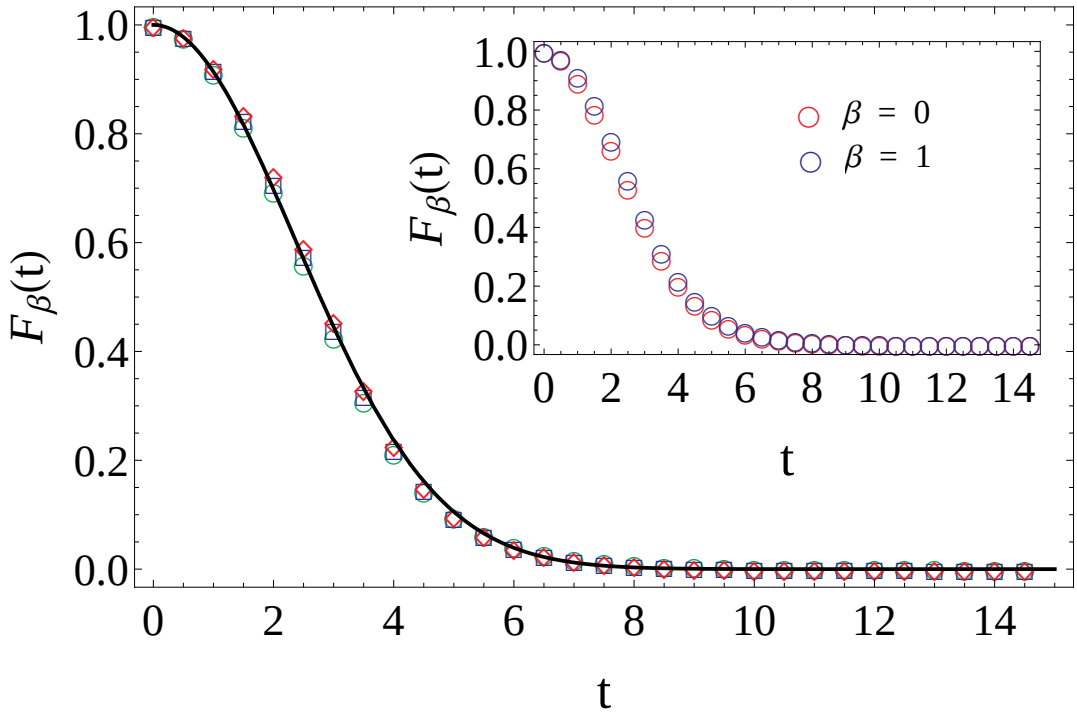

FIG. E.1. OTOC for the fermionic SYK model at infinite temperature. The coupling strength $J_{i,j;k,l}$ has a unit variance. Green circles, blue squares and red diamonds correspond to $N = 15, 16, 17$, respectively. The black solid curve is the best fit to a Gaussian decay. Inset: OTOC for 16 fermions at the same coupling strength at different temperatures.

On the other hand, this observation fits into the theory of the present work: The OTOC decay rate is governed by the coupling strength between the target subsystem S_A, S_B and the rest of the system. In a finite system, the

coupling might be too large for the decay to be in the exponential regime. The decay rate extracted from our numerical simulation is close to the bandwidth (the width of the spectral density) of the SYK Hamiltonian, which indicates that the decay is in the Gaussian regime.

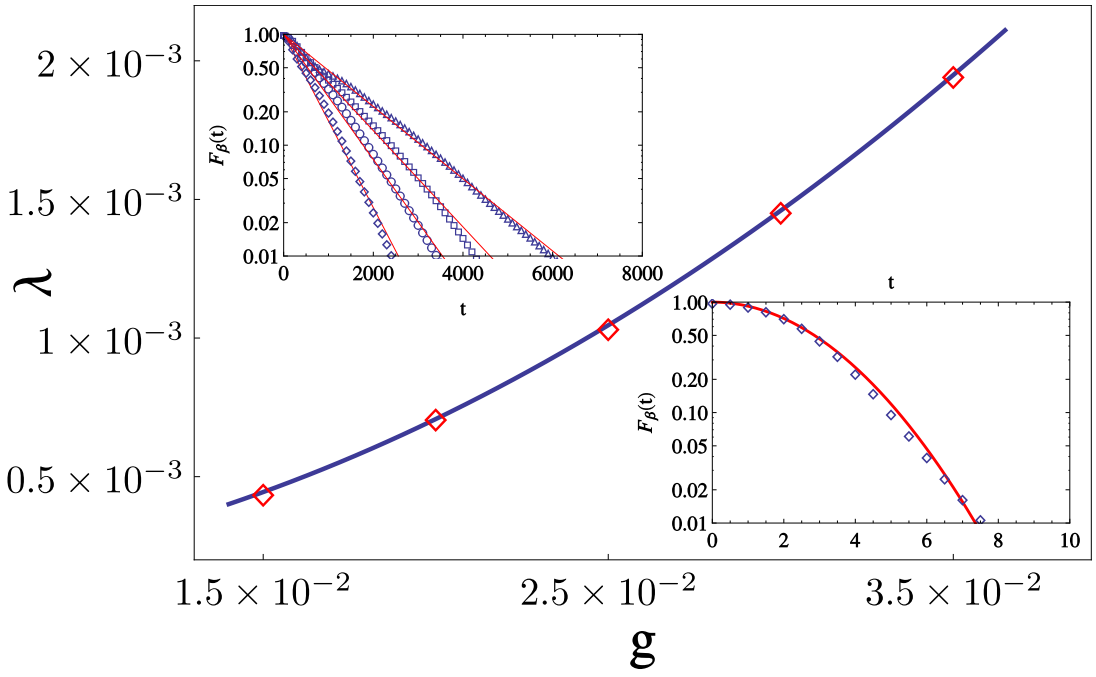

FIG. E.2. Exponential decay rate λ v.s. g factor. The blue solid line is the best fit to the quadratic form. The decay rates are extracted from the numerical simulation of the OTOC evolution for the fermionic SYK model of 16 fermions with manually decreased couplings (by a factor $0 < g < 1$) between the target subsystem and the rest of the whole system, see text for details. Inverse temperature is fixed at zero. The data are obtained by averaging over 50 realizations. The top inset shows typical decay curves at decreased coupling strength. The triangles, squares, circles and diamonds correspond to $g = 0.02, 0.025, 0.03$ and 0.035, respectively. The bottom inset shows the Gaussian decay without decreasing the coupling strength ($g = 1$).

Since the relative strength of the coupling between the two subsystems S_A and S_B compared with the total Hamiltonian decreases with the system size, it is then expected that the OTOC decay would drop into the exponential regime in the large-N limit. Due to the limited numerical capacity, we did not observe exponential decay up to 17 fermions, which is the largest system we are able to simulate numerically. However, we are able to observe exponential decay by manually adjusting the coupling strength. It is done by decreasing the couplings $J_{i,j;k,l}$ that involve the subsystem S_A and S_B by a factor $0 < g < 1$, while keeping the coupling in the rest of the system unchanged.

Figure E.2 shows the exponential OTOC decay for the deformed coupling strength. The decay rate also admits quadratic dependence on the coupling factor g, which satisfies the Fermi's golden rule prediction for the exponential decay of the LE.

[1] A. Bhattacharyya, W. Chemissany, S. Shajidul Haque, and B. Yan, "Towards the web of quantum chaos diagnostics," (2019), arXiv:1909.01894 [hep-th].

[2] A. A. Budini, A. Karina Chattah, and M. O. Cáceres, "On the quantum dissipative generator: weak-coupling approximation and stochastic approach," Journal of Physics A: Mathematical and general **32**, 631 (1999).

[3] J. Maldacena, S. H. Shenker, and D. Stanford, "A bound on chaos," Journal of High Energy Physics **08**, 106 (2016).

[4] N. Tsuji, T. Shitara, and M. Ueda, "Bound on the exponential growth rate of out-of-time-ordered correlators," Physical Review E **98**, 012216 (2018).

[5] T. Gorin, T. Prosen, T. H. Seligman, and M. Žnidarič, "Dynamics of Loschmidt echoes and fidelity decay," Physics Reports **435**, 33–156 (2006).

[6] K. Hashimoto, K. Murata, and R. Yoshii, "Out-of-time-order correlators in quantum mechanics," Journal of High Energy Physics **10**, 138 (2017).

[7] W. Fu and S. Sachdev, "Numerical study of fermion and boson models with infinite-range random interactions," Physical Review B **94**, 035135 (2016).

[8] P. Hosur, X.-L. Qi, D. A. Roberts, and B. Yoshida, "Chaos in quantum channels," J. High Energy Physics **02**, 4 (2016).